Expanded View Figures

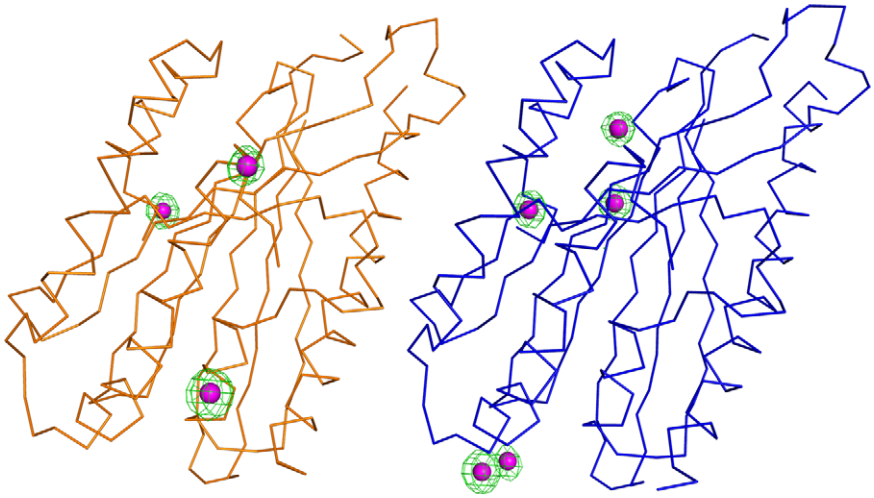

Figure EV1. Anomalous density of I^-.
The densities are contoured at 4 σ and colored in green, and the I^- atoms are shown with magenta spheres; the Cα traces of Ups1-Mdm35 are shown. There are two Ups1-Mdm35 dimers in one asymmetry unit.

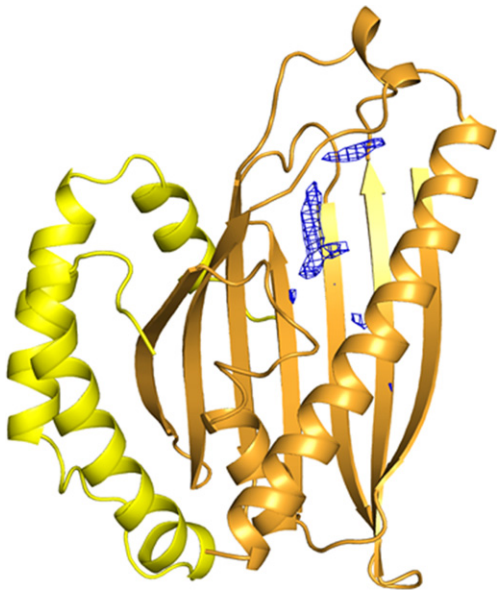

Figure EV2. Fo-Fc electron density map (contoured at 2 σ and colored blue) at the putative lipid-binding site of Ups1-Mdm35 structure.
Ups1 and Mdm35 are shown with ribbon cartoons.

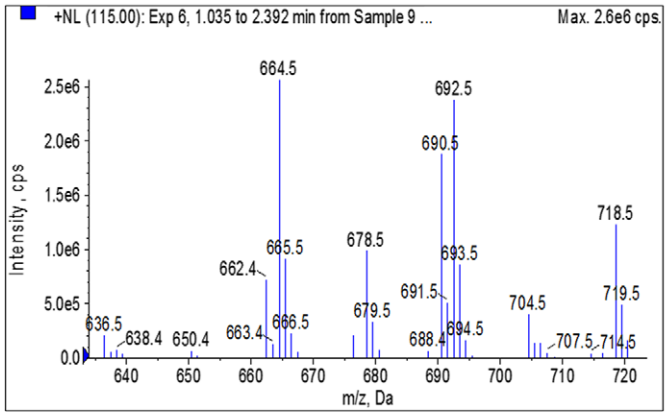

m/z	PA species
636.4	PA 30:1+NH4
638.5	PA 30:0+NH4
662.4	PA 32:2+NH4
664.5	PA 32:1+NH4
666.4	PA 32:0+NH4
688.4	PA 34:3+NH4
690.5	PA 34:2+NH4
692.5	PA 34:1+NH4
694.5	PA 34:0+NH4
692.4	PA 34:1+NH4
714.4	PA 36:4+NH4
716.4	PA 36:3+NH4
718.4	PA 36:2+NH4
720.4	PA 36:1+NH4

Figure EV3. LC-MS analysis result of the lipid composition in the recombinant Ups1-Mdm35 protein complex.
There are various kinds of lipids in the protein complex, of which 32:1 (16:0–16:1) PA and 34:1 (16:0–18:1) PA have the highest content.

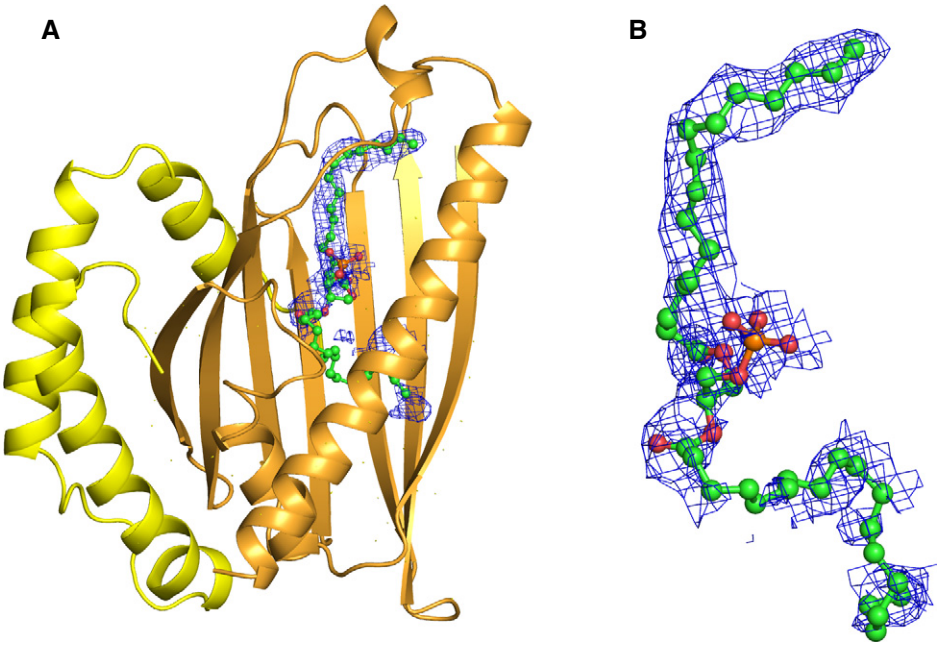

Figure EV4. Electron density map of PA in the Ups1-Mdm35-PA structure.
A Fo-Fc electron density map of PA (shown with green ball and sticks) in the lipid-binding pocket of Ups1 (contoured at 2.0 σ level and colored blue).
B Close-up view of the electron density of PA.

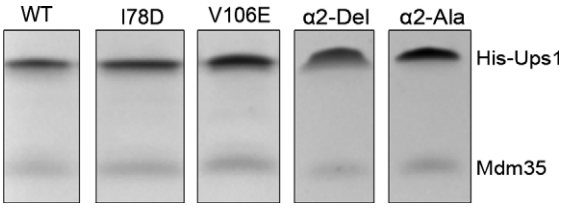

Figure EV5. SDS–PAGE result of Ups1-Mdm35 complex (wild-type and mutations) purification.
The gel is stained with Coomassie blue.

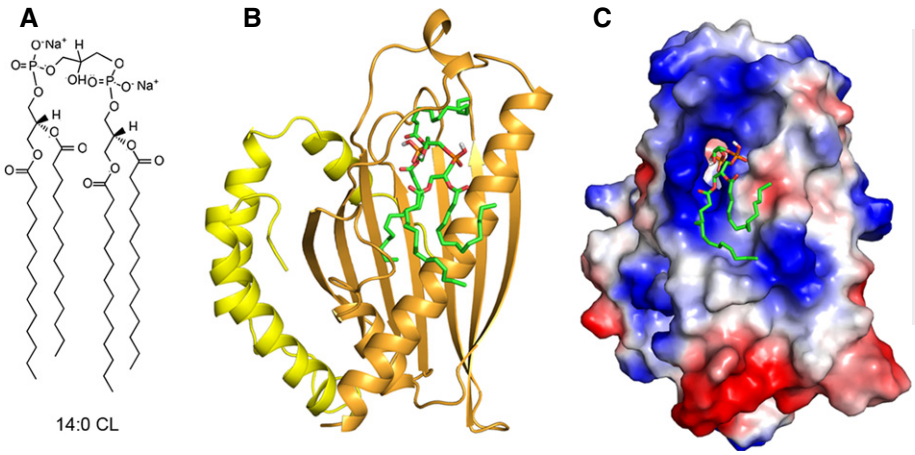

Figure EV6. Possible binding mode of CL with Ups1-Mdm35.

A Chemical structure of CL (14:0).

B Structure model of Ups1-Mdm35 bound with a 14:0 CL. Ups1-Mdm35 is shown with ribbon cartoon, and CL is shown with a green stick model.

C Structure model of Ups1-Mdm35 bound with a 14:0 CL. Ups1-Mdm35 is shown with electrostatic potential surface, and CL is shown with a green stick model.

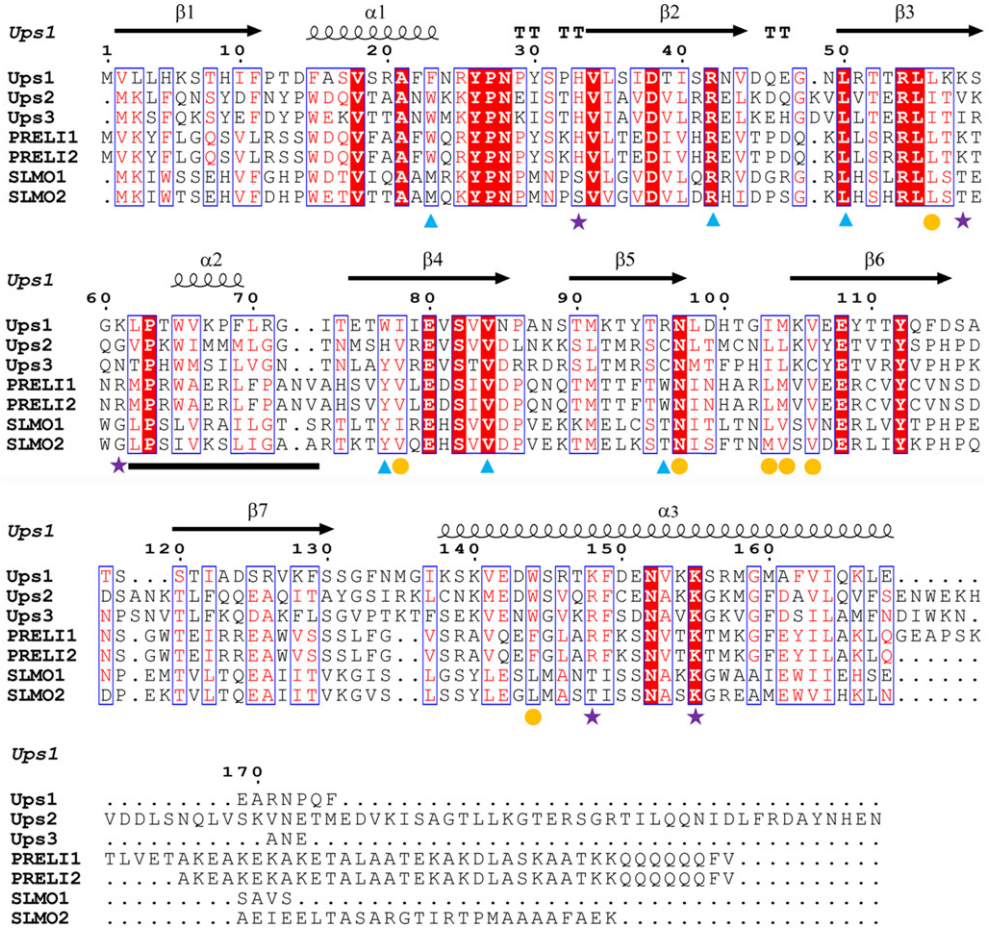

Figure EV7. Sequence alignment of Ups1 homologues.

Secondary structure elements of Ups1 are shown on top. The conserved residues are boxed and colored in red, and the strictly conserved residues are shaded. The residues involving the PA-binding pocket are indicated with orange spheres; the residues constituting the hydrophilic patch are indicated with purple stars; and the residues involving the Mdm35-Ups1 interface are indicated with cyan triangles. The residues constituting the helix α2 are underlined.

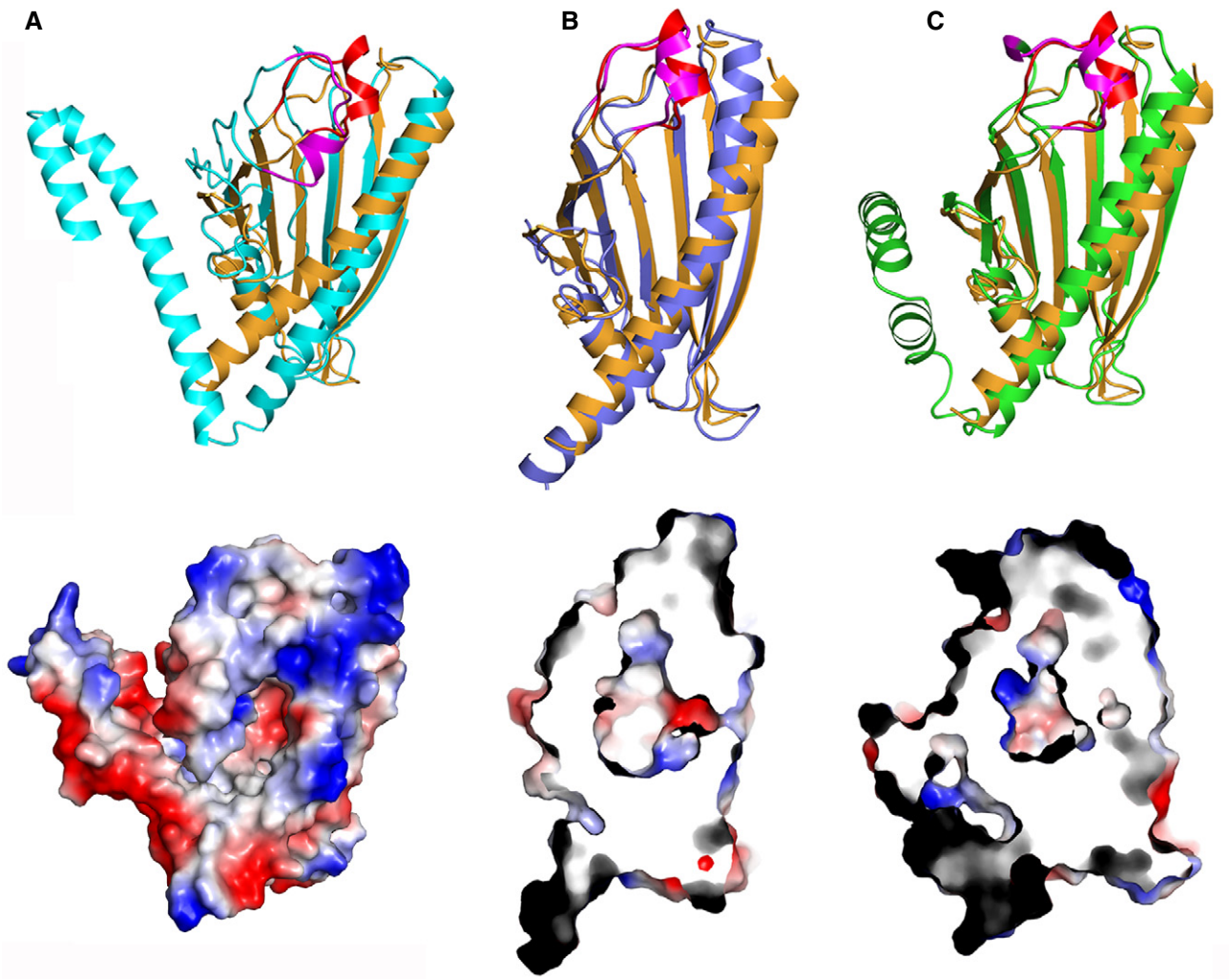

Figure EV8. Modeling structures of Ups2, Ups3, and PRELI1 based on the structure of Ups1.

A–C Upper panel: the structures of Ups2 (A), Ups3 (B), and PRELI1 (C) are shown with cyan, blue, and green ribbons, respectively (α2 helices are colored in magenta). Each structure model is superposed with Ups1 that is shown with orange ribbons (α2 helix is colored in red). Bottom panel: cross section views of the electrostatic potential surface models show the potential lipid-binding pocket in Ups2 (A), Ups3 (B), and PRELI1 (C).

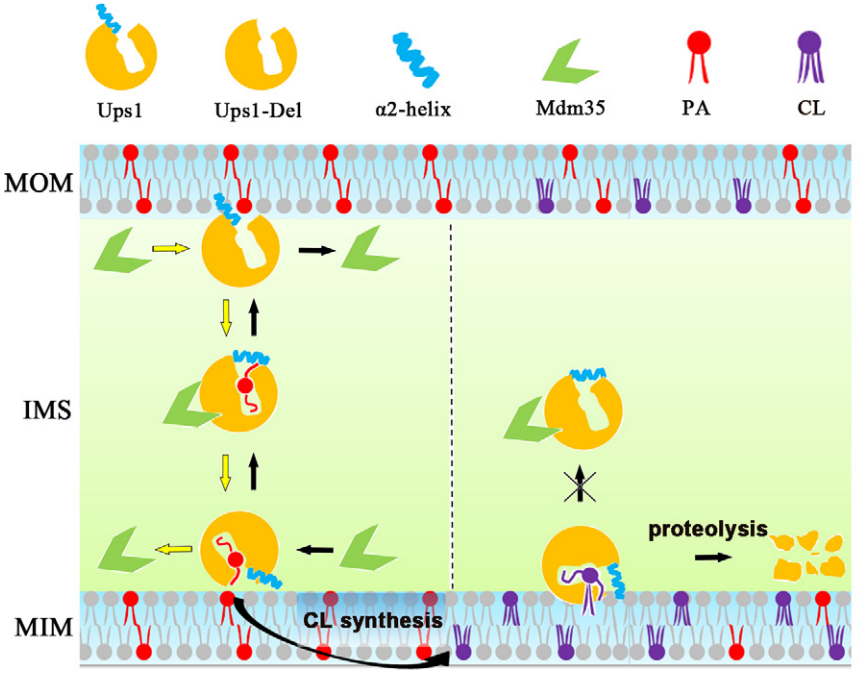

Figure EV9. Model for Ups1-Mdm35-mediated PA transport.
Ups1 may attach to the MOM through charge–charge interactions via hydrophilic patch, which may drive the conformational change of lid α2 to expose the lipid-binding pocket to extract PA from the membrane. Once PA binds into the pocket, α2 will close the pocket. Then, Mdm35 binds with Ups1 to form Ups1-Mdm35-PA complex and dissociates from MOM and translocates PA across the IMS to the MIM. Upon arriving at the MIM, α2 lid opens to releases PA. This process may be dynamic and reversible, and the translocation of PA depends on the higher concentration of PA at MOM than at MIM since the PA is used for the synthesis of CL at MIM. Once the amount of CL is sufficient, CL may capture Ups1-Mdm35 complex at MIM to feedback-regulate PA trafficking.